Stray Light Shielding for Formation Flying X-ray Telescopes

Paul B. Reid[+a], Michael Garcia[a], and Jeffrey Stewart[b]
[a]Harvard-Smithsonian Center for Astrophysics, 60 Garden St., Cambridge MA USA 02138
[b]NASA Goddard Space Flight Center, Greenbelt, MD USA 20771

ABSTRACT

Recent studies and planning for a variety of x-ray astronomy missions (Constellation-X, XEUS, Generation-X) have driven astronomers to explore grazing incidence telescopes with focal lengths of 50 m or greater. One approach to implementing such long focal lengths is to employ formation flying: separate optic and detector spacecraft travel in formation. Formation flying removes the "telescope tube" which was an integral part of shielding the telescope from straylight. We consider the implications of formation flying with respect to straylight, and discuss some design guidelines for baffling the straylight. The Constellation-X mission is used as an example.

Keywords: x-ray optics, straylight, baffling, Con-X, formation flying

1. INTRODUCTION

The potential reconfiguration of the NASA Constellation-X mission and the planned architecture of the European Space Agency's XEUS mission both rely upon formation flying of separate detector and optics spacecraft. Similarly, the NASA Visions Program study mission Generation-X is also envisioned as a formation flying mission. Formation flying offers the advantages of: long focal lengths without the need for an extensible optical bench, replaceable focal planes, and the capability to move different detectors in and out of the field of view. (Formation flying is not without its complications and difficulties, but that is not the subject of this paper). In most formation flying approaches, the two spacecraft are completely physically decoupled from one another. Absent an outer telescope tube, more stringent baffling is required for the aft end of the optics spacecraft and the forward end of the detector spacecraft. This baffling is necessary to control straylight from a variety of sources: the Sun, the diffuse x-ray background (DXB), the Moon and Earth, bright planets, and Zodiacal light.

In all cases, the impacts of straylight are several. It raises the background count rate, thereby diminishing signal to noise ratios and further constraining observation of faint objects. It can damage detectors, reduce their lifetime, and/or increase their internal noise levels. Because the baffling may be more extensive than in the case of an enclosed telescope, baffle impact upon payload weight and packaging needs to be considered. These problems require straylight baffling be included as part of the system design for formation flying x-ray telescopes.

In this paper we will discuss straylight requirements relative to a formation flying version of Con-X/XEUS. We will derive an expression for the required baffling. Lastly, we consider the implications of the baffling for a variety of different configurations of the telescope.

2. STRAYLIGHT SOURCES

The two most significant sources of straylight are the Sun and the DXB. In one case the straylight is predominantly visible and IR, and directed from a single source. In the other case the straylight is in the soft x-ray region (0.2 to 1 keV) and, as its name implies, diffuse in nature.

In the case of the Sun, we are all aware of the perils of direct illumination of a detector by the Sun – clearly the detector must be shielded. In addition, the forward (entrance) end of the mirror assembly (or mirror) must also be shielded.

[+] preid@cfa.harvard.edu; phone 1 617 495-7233; fax 1 617 495-7356

Moreover, there are far too many photons reflecting and scattering off various mirror assembly structure to have any good control over the straylight situation if direct illumination of the forward end of the mirror is allowed. In both cases, shielding must include the desired range in spacecraft pitch and roll angles so as to maintain the efficacy of the shielding for all allowable spacecraft pointing.

Because of the copious amounts of flux from the Sun, we also need to consider light scattered off other structure, including the sun shades themselves. Therefore, we must shield the aft (exit) end of the mirror from direct illumination of the Sun. With less bright sources (planets, Earth, Moon, Zodiacal light) it may be unnecessary to provide this additional shielding against light scattered once or more off of other structure.

Lastly, we must shield against the diffuse x-ray background. Here we note another major difference between formation flying and fixed rigid telescopes. The enclosing telescope outer tube completely baffles the detectors from any view of the DXB other than what falls within the telescope field-of-view (FOV). In formation flying we need to separately supply that baffling. While the DXB does vary over the sky[10,11], in general we treat the DXB as approximately constant. The critical issue here is deciding how much of the sky can be viewed by the detectors before determining the shielding (baffling) required.

3. FORMATION FLYING CONFIGURATIONS

We considered two 50 m focal length formation flying variants. In the first the Con-X segmented Wolter I optics are used[1], but in this case with a 4 m diameter mirror assembly and 350 reflector shells (this configuration would replace the 4 telescope baseline configuration of Con-X). Each reflector is ~ 0.4 mm thick. The detector complement consists of a calorimeter (the XMS[2]) a reflection grating spectrometer (RGS[3]), and possibly a wide field imager such as envisioned for XEUS[4]. The RGS consists of a reflection grating array (RGA) and a set of CCDs functioning as the camera (RFC). A separate zero order camera (ZOC) is also used. Because Con-X is designed as a spectroscopy mission, nominal instrument bandwidths are defined over which spectral resolution exceeds some minimum requirement. For the baseline mission this implies an RGS bandwidth of 0.25 to 0.6 keV (with a lower limit goal of 0.1 keV), and an XMS bandwidth of 0.6 to 12 keV. The RGA may either be mounted directly to the mirror assembly, offering the greatest spectral resolution, or it may be supported on a boom extending from the focal plane. For this configuration we consider only the former. The wide field imager (WFI) would be moved into/out of the beam and has a 5 arc-min on a side FOV and a bandwidth of ~ 0.1 to 10 keV.

In the second variant we use the collaborative approach of a XEUS mirror with a Con-X/XEUS set of detectors. Here too a 50 m focal length was used. The XEUS mirror is ~ 7m by 7m in extent[5]. Approximately 17 per cent of the collecting area is dedicated to the RGS. This telescope employs the same detector suite as above. In addition, for this configuration we also consider the implications of placing the RGA on the detector spacecraft, using an ~ 10 m boom to position the gratings in front of the grating detectors.

4. REQUIREMENTS

Requirements are set by the scientific goal of obtaining spectra of faint astrophysical sources. We require the DXB flux from direct view of the sky to be less than or equal to the DXB flux through the mirror assembly at the detector. With respect to the Sun, Earth, Moon, etc. we require the detector background caused by this straylight to be low enough so as to not degrade the ability to detect and conduct spectroscopy on faint objects.

4.1. Diffuse X-ray Background

We require the DXB flux from direct view of the sky to be less than or equal the DXB flux as collected by the mirrors. We estimated the allowable direct view of the sky consistent with the requirement by:

$$F_{DXB} \cdot d\Omega_{mirror} \cdot A_{RGS} \approx F_{DXB} \cdot d\Omega_{RFC} \cdot A_{RFC} \cdot \varepsilon_{RFC} \qquad (1),$$

where F_{DXB} is the diffuse flux per unit solid angle per unit area, $d\Omega$ is the solid angle, either for the mirror FOV or the allowable solid angle view of the sky for the spectrometer detector RFC, A_{rgs} is the effective area of the RGS, A_{RFC} is the geometric collecting area relevant to the RFC, and ε_{RFC} is an efficiency factor for the RFC/ZOC. Note we assume the DXB flux is uniform over a region of the sky representative of the mirror FOV and its surroundings.

We solve eq. (1) for $d\Omega_{RGA}$.

$$d\Omega_{RFC} \approx d\Omega_{mirror} \cdot \left[\frac{A_{RGS}}{A_{RFC}} \cdot \frac{1}{\varepsilon_{RFC}} \right] \qquad\qquad (2).$$

We can analyze eq. (2) for both the XEUS mirror and the 4 m diameter Con-X mirror. However, the grating area is sized such that both configurations give essentially the same effective area for the grating. We set:

$A_{RGS} = 0.1 \text{ m}^2$
$d\Omega_{mirror} = (2.5 \text{ arc-min})^2 \text{ [Con-X], or } (5 \text{ arc-min})^2 \text{ [XEUS]} = 0.53 \times 10^{-6} \text{ or } 2.1 \times 10^{-6} \text{ ster}$

The values we choose for A_{RFC} and ε_{RFC} are determined by the details of the telescope and instrument configuration. First, we consider the configuration where the grating assembly is mounted directly aft of the mirror assembly. In this configuration, diffuse background x-rays can only be incident directly upon the RGS detector. The equivalent area A_{RFC} for is the area over which the spectra are distributed: approximately 100 pixels in the cross dispersion direction times ~ 700 mm in the dispersion direction. For 30 μm pixels this corresponds to $A_{RFC} = 2.1 \times 10^{-3} \text{ m}^2$. We assume an RFC CCD energy resolution of ~ 50 eV, resulting in detector resolution of ~ 5 at 250 eV. Thus, via pulse height discrimination, we can eliminate more than ~ 80 per cent of the incident straylight photons, arriving at an RFC efficiency ε_{RFC} of 0.2. Substituting this area and an efficiency into eq. (2) yields an allowable direct view of the sky by the RGS detector of ~ 5.1×10^{-4} ster for the XEUS mirror and ~ 1.26×10^{-4} ster for the Con-X mirror. At a distance of 50m from the detector, this is equivalent to a swath of sky ~ 4.5 cm wide around the perimeter of the XEUS mirror or ~ 2.5 cm wide around the circumference of the Con-X mirror. Both these areas are quite small compared to the mirror area and the available sky area. Moreover, we recognize that even this requirement still doubles the sky background relative to that as seen directly through the mirror. In an engineering requirements sense, both these requirements are relatively similar to requiring no direct view of the DXB sky by the detectors.

An alternative configuration of the RGS is to mount the grating assembly on a boom extended off the detector spacecraft. Now we must consider baffling the detectors against the DXB from two "sources": direct view of the sky as before (which is essentially not "allowed"), and direct view of the sky as seen through the RGA. The latter case is equivalent to baffling the input to the RGA to limit its view of the sky. In this case we return to eq. (2), replace A_{RFC} with A_{RGA} – the entrance area of the grating array, and we add an additional efficiency ε_{RGA} term in the denominator of the right hand side of the equation. This term represents the efficiency of the DXB getting through the RGA and ending up in the "right place" on the RFC – that is, the photons must manage to get through the RGA, still be incident upon the detector, and strike the proper range of pixels on the detector corresponding to the spectra location.

For the Con-X/XEUS configurations, $A_{RGA} \sim 0.3 \text{ m}^2$. Substituting for the areas and ε_{RFC} in eq. (2) we are left with:

$$d\Omega_{RGA} \approx 1.6 \cdot d\Omega_{mirror} / \varepsilon_{RGA} \qquad\qquad (2').$$

For $\varepsilon_{RGA} \sim 0.01$, we find $d\Omega_{RGA}$ is required to be less than 3.5×10-4 ster. This implies a band of sky ~ 3 cm wide around the 7 m XEUS mirror. Clearly, some form of baffling is required in this case as well. We return to eq. (2') later.

4.2. Sun, Earth, Moon, etc.

The Con-X faint object requirement is to measure the x-ray spectra of objects with fluxes of 2×10^{-15} ergs cm^{-2} s^{-1} in the band 0.2 to 2 keV in less than 10^5 seconds. For XEUS, the requirement is ~ 4×10^{-18} ergs cm^{-2} s^{-1} in the band 0.2 to 2 keV in less than 10^6 seconds. Assuming an average photon energy of ~ 0.5 keV, and grating spectrometer effective area

of ~ 0.2 m^2 (at 0.5 keV) for either the Con-X or XEUS mirrors, the above flux and integration time are consistent with ~ 5 x 10^{-3} photons/s, or ~ 500 photons for a 10^5 second observation. For the XEUS wide field imager (WFI), the effective area is ~ 10m^2. At the faint object limit the photon flux is thus ~ 250 photons for a million second observation, with half the photons within the 2 to 5 arc-sec HPD.

These faint objects – predominantly (but not limited to) active galactic nuclei (AGNs) at large distances - appear as point sources – their flux is distributed over the telescope point spread function (PSF). We assume a 5 arc-sec half power diameter (HPD) point spread function (PSF). For the RGS, the impact of the PSF plus other aberrations spread the flux in the dispersion direction over a wavelength resolution element $\Delta\lambda$ ~ 450 um wide, and ~ 3 mm high in the cross dispersion direction. Thus an RGS resolution element is ~ 1500 pixels in area, and contains ~ 50 per cent of the source photons. Dispersing the spectrum drops this count rate down to perhaps 1/10th the value, or ~ 25 counts/spectral line. To reliably detect this flux, the visible light background rate needs to be ~ 1/10th this count rate, ~ 10^{-9} background counts/pixel/30 msec integration period, or essentially zero.

The goal low energy bandwidth of the RFC is 100 eV. Given ~ 50 eV energy resolution for the CCD, we set a low energy threshold of ~50 eV. Any amount of energy (charge) collected in a pixel less than this amount is "ignored." Each visible light photon is detected by the CCD, and produces ~ 3.6 eV of energy. We desire no visible light counts in any of the 1500 pixels, each sampled every 30 msec over 10^5 sec, or no stray counts in 5 x 10^9 pixel integrations. This is equivalent to requiring the total energy deposited in a pixel be less than 50 eV at the approximately 7 sigma level. Two visible light photons, including 7 sigma statistics, can produce [2 + 7sqrt(2)] x 3.6 eV = 42.8 eV. Thus, a 50 eV low energy discriminator with 50 eV resolution gives an "allowable" stray visible light background of ~ 2 photons/pixel/integration period. This results in essentially zero stray visible light background. We use this 2 photon limit as our requirement in the following discussions.

For the XEUS Wide Field Imager (WFI) the integration period is 5 ms and the pixel size is ~ 75 um. Using similar methodology as above but without dispersive spectroscopy, and using the XEUS faint object requirement, this produces a count rate of ~ 10^{-8} to 10^{-9} source photons/pixel/integration period, similar to that of Con-X. Given a desired 50 eV low energy limit for the WFI, we use a visible light count rate still on the order of 0.5 visible photons/pixel/integration period with an ~ 25 eV LLD.

5. BAFFLING THE DIFFUSE X-RAY BACKGROUND

As in Section 4.1 we consider two configurations for diffuse x-ray background baffling: the RGA on the mirror space craft, and the RGA mounted on the detector space craft approximately 10 m forward of the focal plane.

5.1. RGA on the Mirror Spacecraft

We consider first the case of the RGA mounted directly to the aft side of the mirror. We derive an equation governing the axial length and radial extent of the required baffles. We refer to Figure 1, a schematic of the telescope. In the figure the mirror exit aperture is shown on the left, with an detector of width w offset from the optic axis by a distance d shown on the right. A mirror baffle of length L_m, offset radially from the mirror by a distance Δr is shown on the right. The extreme ray from the mirror is the ray from the edge of the mirror aperture that intersects the edge of the detector. As the detector is sized to accommodate some field of view, the detector width $w = FL \times FOV$, where FL is the mirror focal length (we use 50 m) and FOV is the desired detector angular field of view (diameter). Note, it may be desired for a variety of reasons to make the detector over-sized, that is, larger than is indicated by the FOV. In that case, the actual value of w would substitute for the value calculated from focal length and field-of-view. However, the area included within the FOV is completely unvignetted in this derivation and every spot on the detector has a clear view to the full mirror. Lastly, we note that the detector may be offset from the optical axis by some distance x_{off}. If the detector baffle goes from the focal plane to point 'A' in Figure 1 it will block all direct view of the sky to the detector (assuming of course the figure is rotationally symmetric about the optical axis). Alternatively, the detector baffle can block the straylight ray anywhere along its path from point 'A' back to the mirror baffle. Solving for the intersection of the two rays at point A, The minimum baffle length for the detector L_d, as a function of the detector width w, mirror diameter d, mirror baffle length L_m and baffle offset Δr, and detector offset x_{off}, is found by:

$$L_d = \cfrac{w}{\cfrac{R + \Delta R - x_{off} + w/2}{FL - L_m} - \cfrac{R - x_{off} - w/2}{FL}}$$
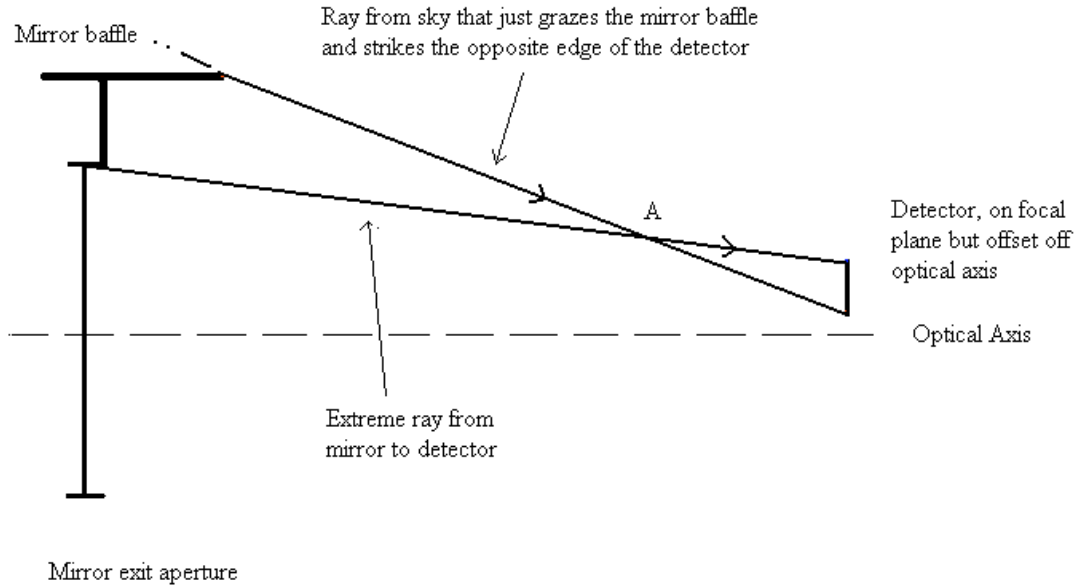
(3).

Figure 1.- Schematic view of mirror, detector, and mirror baffle. The extreme ray from the mirror represents the edge of the mirror aperture and the edge of the field-of-view accommodated by the detector. Note the detector is also offset from the optical axis, in this figure. The straylight ray just grazes the edge of the mirror baffle and strikes the opposite edge of the detector. To eliminate direct view of the sky the detector baffle must intersect the straylight ray at point A, or somewhere along the line joining point A and the mirror baffle.

From eq. (3), if the mirror baffle length is zero (i.e., the mirror baffle is just a "skirt" surrounding the mirror), then eq. (3) reduces to:

$$L_d = \frac{w \cdot FL}{\Delta R + w} \approx \frac{w \cdot FL}{\Delta R} \quad \text{for } \Delta R \gg w$$

(3').

Thus employing only a mirror skirt, the detector baffle length increases approximately linearly with FOV, and varies inversely with the radial width of the skirt. This is seen in Figure 2 where detector baffle length is plotted as a function of on-axis detector FOV. Note that there is no sensitivity in this case to whether the detector is located on or off-axis, and there is also no sensitivity to the size (diameter) of the mirror.

We examined the case where the mirror baffle is a combination of a radial skirt and an axial baffle (Figure 3). Here we observe that the detector baffle length can be significantly reduced by the addition of the radial skirt. Going from a "zero" width skirt to a 2 m wide skirt, along with a [fixed] 2 m long mirror baffle, reduces the length of the detector baffle by about an order of magnitude for the parameters we used (representative of Con-X and XEUS). We also see in figure 3 that the with the inclusion of the mirror axial baffle, the larger XEUS mirror actually requires a shorter detector baffle than the Con-X mirror.

We looked at the impact of varying the length of the mirror axial baffle (with a fixed 250 mm wide skirt baffle) on the length of the detector baffle, as shown in Figure 4. We see increasing the mirror baffle length reduces the detector baffle length, although not as dramatically as the addition of a radial skirt as shown in Figure 3.
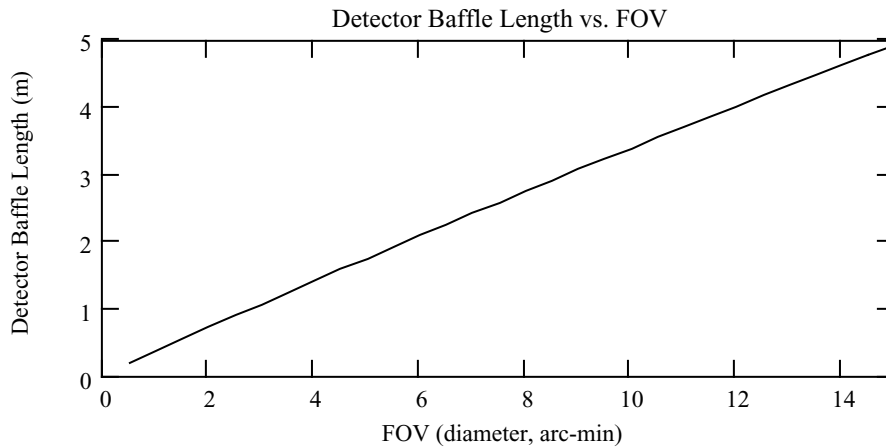
Detector Baffle Length vs. FOV

Figure 2.- Detector baffle length as a function of detector field of view. This case was run for a 2 m wide mirror skirt baffle and a 50 m focal length mirror.
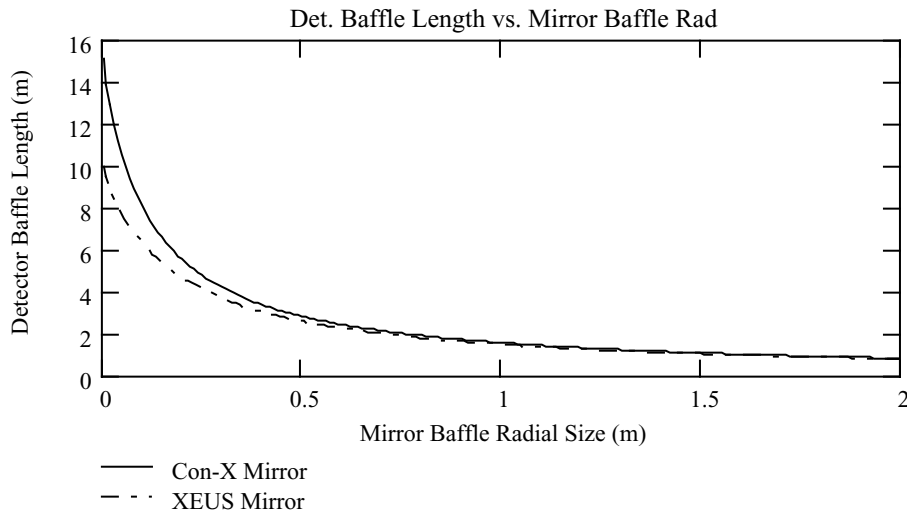
Det. Baffle Length vs. Mirror Baffle Rad

———— Con-X Mirror
— · · XEUS Mirror

Figure 3.- Comparison of 4 m diameter Con-X and 7 m "side" XEUS mirrors, both with a fixed axial mirror baffle 2 m long, a 2.5 arc-min FOV detector, and the radial width of the mirror "skirt" baffle is varied.

Given that the two spacecraft are flying in formation, there may be some interest to determine the combination of mirror and detector axial baffle lengths that gives the minimum total baffle length. Such a configuration maximizes the distance between the two spacecraft, which might be advantageous for formation flying (e.g., minimizing any risk of collision). In Figure 5 we plot the sum of the two baffle lengths as a function of mirror baffle length. We see that the minimum configuration occurs when the mirror and detector axial baffle lengths are equal to one another.

Lastly, we consider the case of rather large detectors as exist with the dispersive RGS. In the baseline 50 m configuration with the RGA mounted on the mirror spacecraft, the RGS has a maximum wavelength of 50 Angstroms, and uses a ruling density of ~ 2900 mm^{-1}. This implies an RFC detector ~ 725 mm long (equivalent to a FOV in Figure

2 of ~ 50 arc-min)! Figure 6 plots the detector baffle length required to shield very long RGS detectors. Clearly, very large baffles become required to control straylight when dispersive spectrometers employ large detectors.

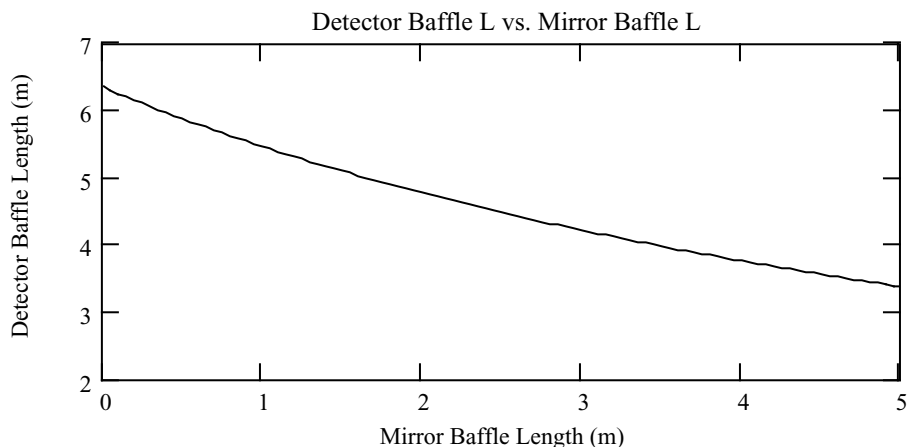Detector Baffle L vs. Mirror Baffle L

Figure 4.- Detector baffle length as a function of mirror axial baffle length with fixed mirror skirt baffle width. We used a 0.25 m wide skirt baffle and a 2.5 arc-min FOV on-axis detector. As usual, the focal length was 50 m, and we used the 4 m diameter Con-X mirror.
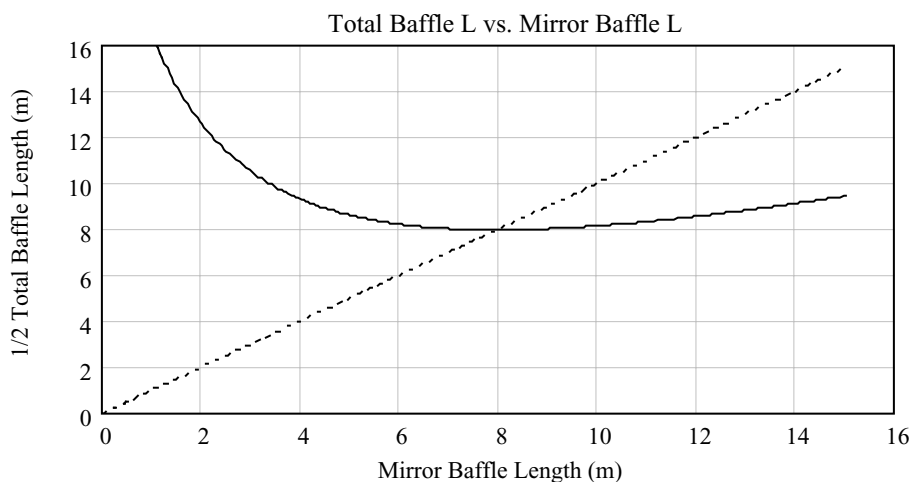
Total Baffle L vs. Mirror Baffle L

Figure 5.- One-half the total axial baffle length as a function of mirror baffle length. There is no mirror skirt and the on-axis detector FOV is 5 arc-min. The dotted line shows equal mirror and detector baffle lengths.

5.2. RGA on the Detector Spacecraft

A second formation flying configuration is under consideration, as previously described. In this case the gratings are carried on a boom, ~ 10 m long, that attaches to the detector spacecraft. Thus the gratings are approximately 10 m forward of the focal plane. There are reasons other than straylight where this configuration may offer benefits over that of the gratings on the mirror configuration.

As before we still need to limit the DXB straylight to the detector. This configuration introduces no changes with respect to shielding the detector relative to the configurations described in the preceding section.   However, because the distance from the dispersing gratings to the focal plane is reduced, and because we presumably cannot arbitrarily increase the grating ruling density to compensate, the size of the detector for the dispersed spectrum decreases. This
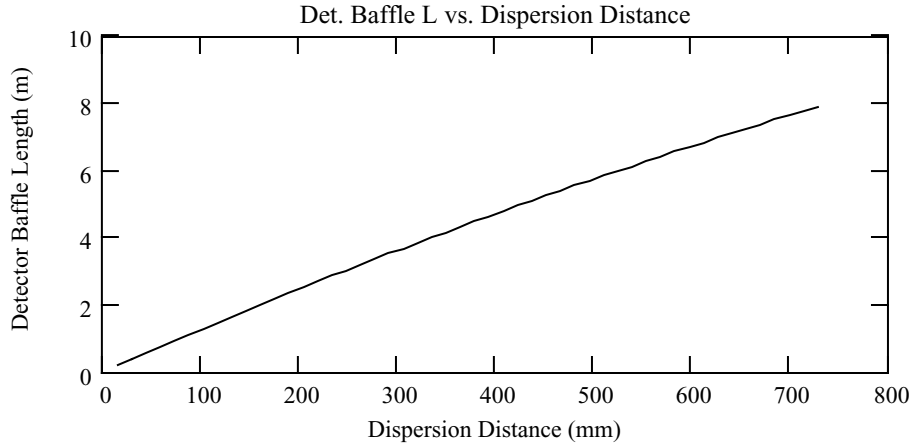
Figure 6.- Detector baffle length for large on-axis detectors for dispersive spectroscopy. In this case the mirror was 4 m in diameter (Con-X), and a 3 m wide radial mirror skirt was employed. The mirror axial baffle was 7 m long. We see that very large baffle sets are required for such large detectors.

reduces the size of mirror and detector baffles required compared the those of Sect. 5.1 For example, if we consider the case where the ruling density doubles to 5800 mm^{-1}, and the distance from grating to detector is reduced to 10 m, the detector size reduces to ~ 290 mm. We recalculate the required baffles and compare the two cases in Table 1. a significant reduction in mirror baffle sizes is achieved along with a not insignificant reduction in detector baffle size.

Parameter	Grating on Mirror	Grating on Detector Boom
Ruling Density (/mm)	2900	5800
Distance to Focal Plane (m)	50	10
Detector Size (mm)	727	290
Mirror Skirt Baffle (m)	3	2
Mirror Axial Baffle (m)	7	0
Detector Axial Baffle (m)	7.9	6.4

Table 1.- Comparison of baffle requirements for two different grating configurations. Both employ the 4 m diameter Con-X mirror.

In addition, we must also consider shielding the entrance aperture of the RGA from the DXB, as shown in Figure 7. Two approaches present themselves: (1) place additional baffling forward of the RGA to provide the shielding, and (2) use fan shaped collimators to baffle the RGA with some [small] loss of efficiency. To calculate the baffle lengths required we just use eq. (3) where we replace the focal length FL by the (e.g.) 40 m separation between the gratings and the mirror. Because the RGA is still relatively large (> 0.5 m in extent), quite long baffles (~ 10 m) need to be attached to the gratings and mirror in addition to the baffles on the detector.

The alternative is the use of fan shaped slat collimators. Because the mirror produces a converging beam, it is possible to design and build a collimator where all the plates lie along the surfaces of "concentric" cones that all have the same vertex (the on-axis focus). Radially directed slats would add stiffness and rigidity to the collimator. If the walls are reasonably thin, and the plates of reasonable length (say ~ 0.5 m) such construction would be feasible. Because all the collimator plates lie along cones with their vertex at the focus, the loss of efficiency is small – the fractional area of the collimator walls relative to the grating assembly entrance area.

The issue with this approach is scattering and reflectance off the collimator walls by soft x-ray background photons. Diffuse x-rays may impinge on the collimator plates at a graze angle as small ~ 4 deg. At energies less than 400eV, reflectance can be as high as 4 per cent or 0.1 per cent or lower depending upon the surface condition. At the low reflectance end, the collimators are efficient enough to alleviate the need for large RGA baffles. At the high reflectance end, they likely allow to much DXB to get to the detectors, impacting the ability to do soft x-ray dispersive faint object spectroscopy. The alternative is decreasing the spacing between collimator plates such that multiple reflection/scattering is required, but this can result in significant loss of throughput both on and off-axis, impacting faint object spectroscopy. The issue of collimators needs to be examined more fully and is work that we plan on undertaking.
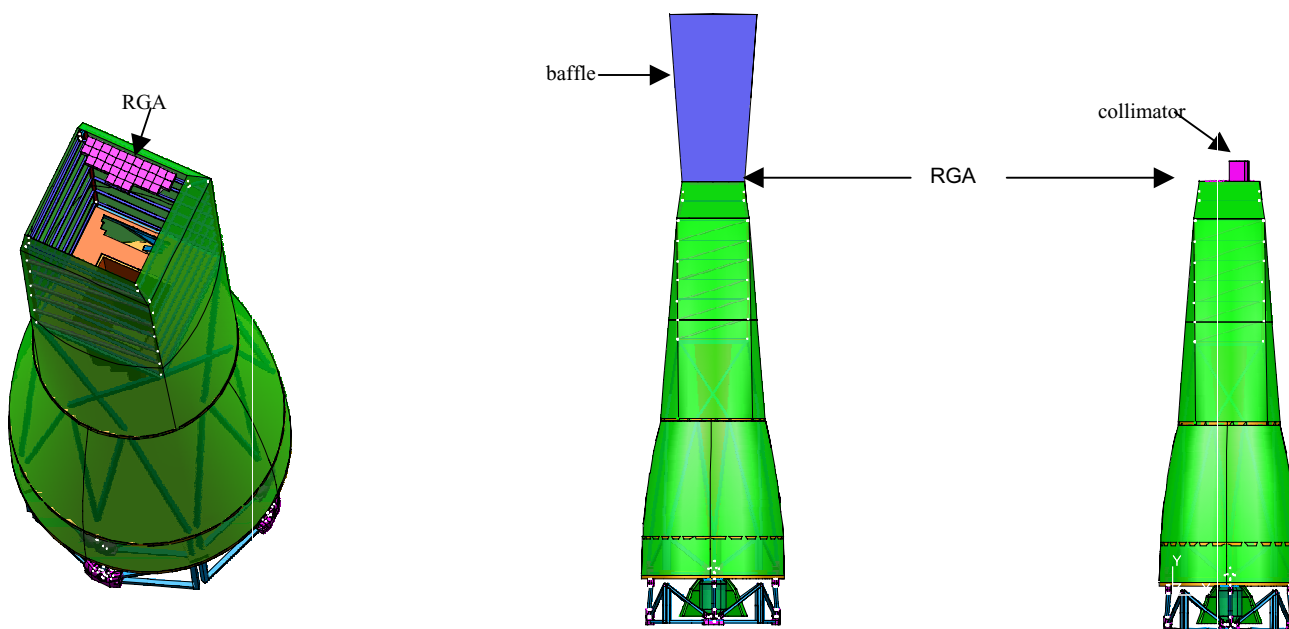

Figure 7.- RGA on the DSC including view of aperture opening and RGA, a view of the RGA on the DSC with baffle and a view of the RGA on the DSC with a collimator.

6. SHIELDING AGAINST VISIBLE LIGHT

We consider the cases of direct illumination by the sun of the detector, aft end of the mirror assembly, aft edge of the optics sun shield, and forward edge of the detector sun shield. For the last three cases, we estimate the flux scattered onto the detector. After estimating the flux incident upon the detector, we estimate the required optical blocking filter in the absence of effective shading. Finally, for the case of scattering off the aft end of the optics spacecraft sunshade, we also estimate what size sunshades (optic and detector spacecraft) are required so as to shield the detector from this straylight. In this manner we can trade off sunshade size versus blocking filter thickness and impact upon effective area.

6.1. Solar flux

The number of photons incident per unit area per unit time from the Sun is given as the solar constant $C = 1370$ Watts-m^{-2} divided by the average energy per photon. We have used 2.5 eV which is more representative of the peak of the black body spectrum for 5800 K, but this is close enough. Upon appropriate unit conversions this results in a flux $F_{solar} = 3.4 \times 10^{17}$ photons-cm^{-2}-s^{-1}. From Sect. 4.2 we desire to reduce this flux to less than ~ 2 to 0.5 photons-pixel^{-1}-integration period^{-1}, or approximately 7.4 to 1.8 x 10^6 photons-cm^{-2}-s^{-1}.

6.2. Direct Illumination of the Detectors and Mirror

Direct illumination of the detectors by the sun is considered unallowable. We primarily concern ourselves with the RGS CCDs and the XEUS WFI because these are the primary low energy instruments. Given an RFC pixel size of ~ 30 um and integration time of 30 milli-sec, and a WFI pixel size of ~ 75 um and integration time of 5 milli-sec, direct solar illumination results in ~ 10^{11} photons/integration period/pixel. Thus both detectors require a sun shade. The minimal size detector sun shade must be large enough to handle the telescope pitch limits of +/- 30 deg. (Con-X) to +/- 15 deg (XEUS), and in simplest form, will be placed at the periphery of the detector spacecraft.

In Section 5 we had already concluded that the detectors could have no direct view of space so as to limit DXB straylight. Thus the DXB baffling also serves to shield against solar illumination. Perrygo et. al.[6], however, also considered damage due to micro-meteoroids. They estimated that for deployable lightweight sunshades for JWST such damage will produce ~ 1 per cent transmissive shields. Even that level of transmission is too high (~ 10^9 photons/integration period/pixel), implying robust, durable sun shades to directly shield the detector from the sun, or, alternatively, multiple layered, spaced shades where only micro-meteoroids traveling towards the detector from the sun produce a pinhole allowing sunlight in towards the detector (see Perrygo).

Direct illumination of the forward end of the mirror allows a plethora of surfaces to reflect and scatter solar flux back toward the detector. As is standard practice, a sun shade is employed at forward end of the mirror. As for the detector shades, they must be sized to accommodate the telescope pitch limits, and similarly robust to micro-damage as above. we also note that the sunshades are beveled at an angle equal to or greater than the spacecraft pitch limits so as to avoid illuminating the inside of the shade and adding a source of straylight.

6.3. Scatter from the Aft End of the Mirror Assembly

In the absence of a sun shade on the aft end of the optics space craft, the aft end of the mirror assembly can be directly illuminated by the sun. Based upon optical and mechanical models of the Con-X mirror assembly, we estimated there exists ~ 1.4 m^2 of surface with an albedo of ~ 4 per cent available to scatter light back towards the detectors. (This area would be larger for the XEUS 7m optic). This results in a scatter flux of ~ 2 x 10^{20} photons/s. The flux per pixel is reduced by the solid angle subtended by a pixel:

$$F_{res} = F_{mirror} \cdot \frac{A_{pix}}{2 \cdot \pi \cdot FL^2} \cdot dt \tag{4},$$

where dt is the integration time, A_{pix} is the pixel area, and F_{mirror} is the stray visible light flux from the mirror. The resulting flux per pixel is ~ 3.3 x 10^5 photons/integration period. (The WFI pixel area is 6.25 times that of the RFC, but its integration time is 1/6th that of the RFC. The combination yields essentially the same flux per pixel per integration time). If an MLI blanket covers the aft end, we can expect higher scattered flux levels due to glints and specular reflection off the MLI.

To reach the required straylight levels, we must either shield the aft end of the mirrors from sunlight, or attenuate the scattered light by factors of ~ 1.7 to 9 x 10^5. This corresponds to ~ 12 to 14 optical depths. Good broadband rejection is achieved with a 1/e depth of aluminum on silicon of ~ 100 A of Al + 40 Angstrom of silicon. Thus, in the absence of effective sun shading we require ~ 1200 A of Al and 400 A of Si for the RFC and 1400 A of Al (+ 400 A Si) for the WFI to eliminate solar stray light from the detectors. Unfortunately, x-ray transmission of these optical blocking filters (OBF) can also be quite low near the detector low energy limits: at 120 eV the respective transmission is 4.7 x 10^{-3} and 8.8 x 10^{-3}. The x-ray transmission for the two thicknesses of Al are shown as a function of energy in Figure 8.
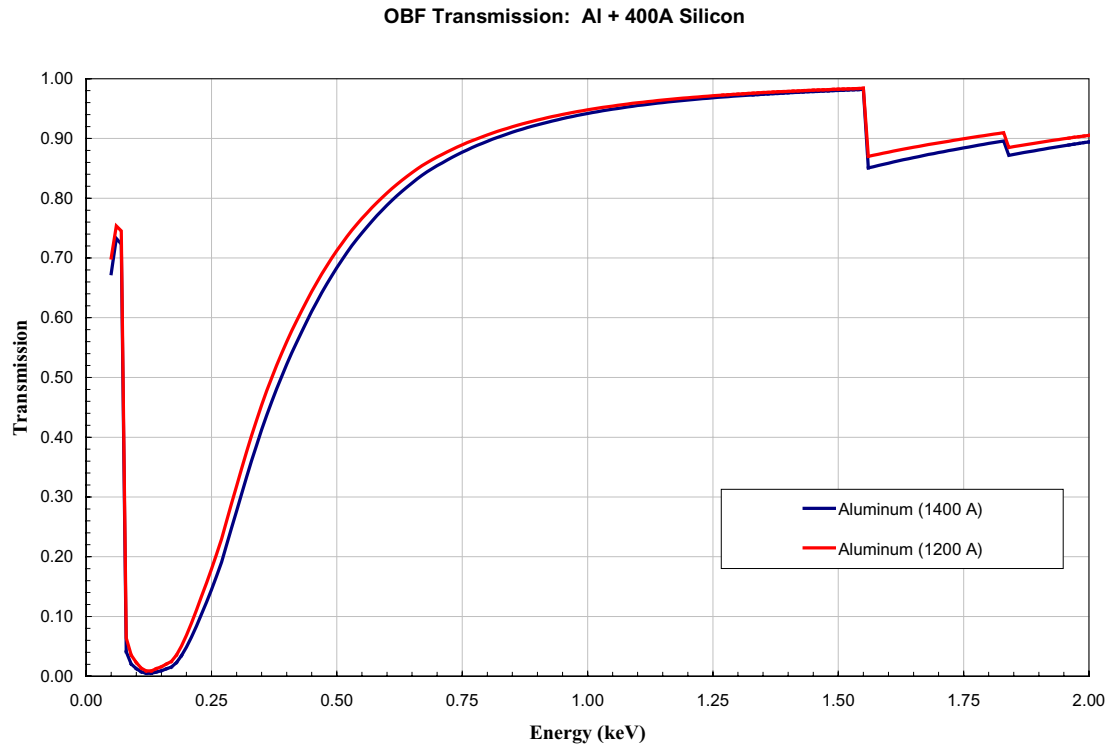
OBF Transmission: Al + 400A Silicon

Figure 8.- OBF transmission for a variety of thicknesses of Al + Si.

We separately modeled the effective area and determined that such thick optical blocking filters attenuate the soft x-ray flux too greatly to achieve effective area requirements at those energies. For example, we estimate that these filter result in achieving only ~ 15 per cent of the Con-X required effective area at 0.25 keV, and ~ 20 per cent of the XEUS effective area goal at the same energy. Thus such thick filters are impractical for faint object soft energy spectroscopy. We therefore also require sun shades on the aft ends of the telescope mirror, similar to those at the forward end.

6.4. Scatter from the Aft End of the Mirror Sun Shade

Once we have established the need for mirror sunshades we consider if there are any additional constraints on them. One area of concern is that sun light will scatter off the aft edge of the sun shade and be incident upon the detectors. This can be avoided by using substantially longer sun shades at detector and optic ends, but the first question is whether this is at all a problem.

Similar to Section 6.3, we estimate the edge area of the sun shade, estimate its albedo at 0.1, calculate the scattered flux, and then account for the solid angle subtended by the detector. Note that in estimating the sun shade edge area we include the requirement that the telescope be free to roll about its optical axis by some amount.

To estimate the edge area, we use two possible shade thicknesses – 0.1 cm and 1 cm. This results in a scattered solar flux off the aft end of the sun shade of ~ 2×10^{18} to 2×10^{19} photons/sec (depending upon sun shade thickness). The flux incident upon the detector is calculated as in eq.(4) but with the length term *FL* is replaced by *FL-shade length*. The resulting flux at the detector within a pixel is ~ 5×10^{3} to 5×10^{4} photons/integration period, requiring optical blocking filters of ~ 9 to 11 optical depths. These correspond to 900 to 1100 A of Al plus 400 A of Si. These thicknesses blocking filters still result in falling short of low energy effective area requirements by about a factor of 3.

We draw the conclusion that shielding against straylight from the Sun requires sufficiently large sun shades on both the detector and mirror space craft so as to satisfy both the condition that no direct light falls on either the aft end of the mirror or the detector, and such that the detector has no direct view of the very aft edge of the mirror sunshade. This last

condition is essentially the same as the requirement that the detector has no direct view of the sky. Thus the baffling approach discussed in detail in Section 5 provides the solution to the solar shielding problem. The only difference is that the sunshields need only baffle in the sun direction, whereas the DXB baffles cover the full 360 degrees of azimuth.

6.5. The Moon, Earth, Bright Planets, and Zodiacal Light

Constellation-X, as would be XEUS or other formation flying x-ray telescopes, will be situated at L2 (the second Earth-Sun libration point), minimizing the station keeping fuel requirements. L2 lies in the plane of the Earth's orbit, approximately 1.6 million km behind the Earth (away from the Sun). This position presents some advantages from a straylight viewpoint: the spacecraft can never see a "full" Moon or Earth, only crescents, reducing the straylight load from these objects. In addition, because the detector is baffled (for the DXB) such that it has no direct view of the sky in any direction, we need only consider indirect sources of straylight – scatter off the mirror baffle and edge or off the aft end of the mirror.

The Earth and Moon, being reasonably close in the sky with respect to the Sun from the viewpoint of L2, are mostly baffled by the sunshields. Flux from the Earth can be eliminated by slightly increasing the size of the sunshields to accommodate a slightly larger pitch range (by an additional ~ 3 to 5 deg.). The full Moon is ~ 14 apparent visual magnitudes fainter than the Sun[7,8] (-12.7 vs. –26.7). This implies a flux that is ~ 2.5×10^{-6} times that of the Sun. Accounting for the fact that L2 is approximately four times further from the Moon than is the Earth, and the fact that at L2 less than a half moon is visible, the lunar flux is less than ~ 10^{-7} times the solar flux. It is possible, given the lunar orbit and spacecraft orbits about L2, for the Moon to illuminate some of the aft end of the mirror even though it is shielded from the Sun. This fraction (~ ½ to ¾) is a function of the pitch angle for which the sunshade was designed. But, with a flux ~ 10^{-7} times that of the Sun, this will produce fewer than ~0.03 photons/pixel/integration period. It is also possible for the Moon to partially illuminate the forward end of the telescope mirrors depending upon the line of sight. This case is eliminated by selecting an observing plan where this does not occur, limiting telescope pitch and yaw pointing at certain points in the lunar cycle. Alternatively, increasing the length of the baffles by ~ $d*\tan(\phi)$, where d is the diameter of the baffle and ϕ is the field angle to the Moon at worst case of lunar and spacecraft orbits, also eliminates this issue.

For the bright planets, Venus, Jupiter, and Saturn, there is also too little flux to be an issue, once we have already shielded the detectors from direct view of the straylight source. Venus has a maximum visual magnitude of –4.4[7], and Jupiter of –2.7[7]. Jupiter, on the other side of L2 from the Sun, has an unimpeded view of the aft end of the mirror and baffle edge. But with ~ 2.5×10^{-10} times the solar flux, the light scattered off the mirror spacecraft result in only ~ 0.002 photons/pixel/integration period. Venus, approximately 5 times brighter than Jupiter, also results in a very low visible straylight flux at the detector.

Lastly, we consider Zodiacal light. Zodiacal light, produced by scattering of sunlight by dust in the solar system, is brightest in the plane of the ecliptic and near the Sun. The Zodiacal light flux is ~ 1.1×10^{-7} ergs-cm^{-2}-s^{-1}-sr^{-1}-A^{-1} over a bandwidth of ~ 3800 to 5500 A[9], and has a solar-like spectrum. Integrating over bandwidth and 2π steradians, allowing for scatter off the aft end of the mirror and the mirror baffles, results in ~ 0.04 photons/pixel/integration period.

Therefore we see that, relative to visible straylight requirements, solar system sources (excluding the Sun) have insufficient brightness when they are able to only indirectly illuminate the detector. And, as a result of shielding against the DXB, no straylight source can directly illuminate the detectors. Thus with shielding against the DXB and shielding against solar straylight, other solar system sources are too faint to be problematic at Con-X and XEUS sensitivity levels.

7. CONSTELLATION-X IMPLEMENTATION

As described above, two 50 m formation flying variants considered include the Constellation-X SXT MSC with the RGA mounted to the back of the mirror and the ESA MSC with the RGA mounted on the DSC are shown in Figures 9 and 10 respectively. Currently, implementing both requires the use of the lift and size capabilities of a Delta IVH or similar launch vehicle with a 5m diameter fairing. Depending on the variant and whether baffles or collimators are utilized, the constraints of the launch vehicle may necessitate the use of a deployable truss to obtain the required length for either the baffle, the RGA distance from the detector or both.
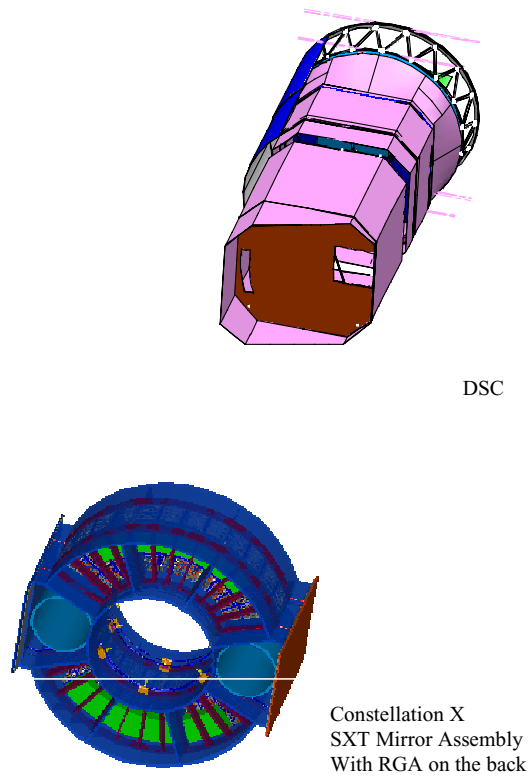
DSC

Constellation X
SXT Mirror Assembly
With RGA on the back

Figure 9.- 50 m Formation Flying Constellation-X SXT Mirror Assembly and DSC
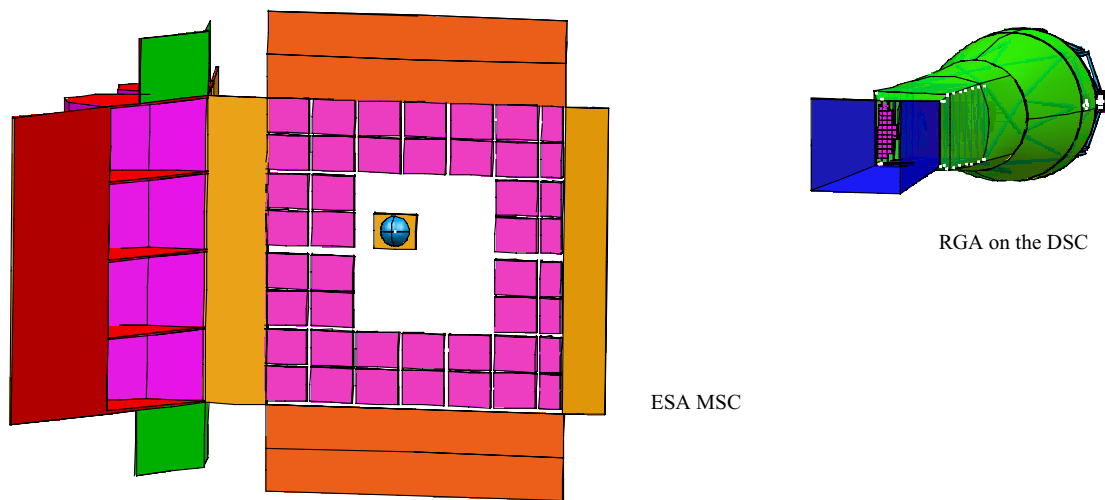

RGA on the DSC

ESA MSC

Figure 10.-50 m Formation Flying ESA MSC with the RGA on the DSC

8. SUMMARY AND CONCLUSIONS

We have considered the stray light environment of a formation flying implementation of the Constellation-X mission. The formation flying configuration utilizes a telescope and detector spacecraft separated by 50m. In order to carry out

the scientific program of observing faint X-ray sources, the detectors must be shielded from direct illumination from the diffuse X-ray background. In addition, the detectors and mirror must be shielded from direct illumination from the sun, and sunlight glinting off the back end of the mirror spacecraft and/or shields must not be allowed to directly enter the detector.

These requirements can be met with sunshades of moderate size (4m to 8m) on both the mirror and detector space-crafts. The exact size depends upon the details of the implementation. It is likely that something on the order of 20% of the space between the 2 spacecraft will be occupied by sunshades. The remaining 40m separation must be maintained by the formation flying system in order to avoid damaging the shades. Impact damage to the shades could result in loss of much of the scientific utility of the mission. In addition, micro-meteorite impacts on the shades must not allow sunlight to 'leak' through, a requirement which may be possible to meet via multi-layered shades.

While not discussed herein, collimators are not a viable alternative for the case with the gratings mounted directly upon the mirror spacecraft, as they have too low a throughput. In the configuration with the gratings mounted 10m in front of the detector spacecraft, collimators may be a viable alternative for shades, which would result in increasing the effective separation of the 2 spacecraft. However, the scattering of X-rays from the diffuse background off these collimators needs to be considered in detail in order to determine their viability.

9. ACKNOWLEDGMENTS

10. REFERENCES

1.   Petre, R., *et. al.*, "The Constellation-X spectroscopy X-ray Telescope," SPIE Proc. **5488**, 505 (2004).

2.   Whitehouse, P.L., Shirron, P.J., and Kelley, R.L., "The X-ray micro-calorimeter spectrometer (XMS): a reference cryogenic instrument for Constellation-X," *Cryogenics*, **44**, 543 (2004).

3.   Flanagan, K., *et. al.*, "The Constellation-X RGS options: raytrace modeling of the off-plane gratings," SPIE Proc. **5488**, 515 (2004).

4.   Lumb, D., "XEUS Mission: detector spacecraft instrumentation package," SPIE Proc. **5488**, 539 (2204).

5.   Bavdaz, M., *et. al.*, "Development of x-ray optics for the XEUS mission," SPIE Proc. **5539**, 95 (2004).

6.   Charles Perrygo, *et. al.*, "Passive thermal control of the NGST", SPIE Proc. **3356**, 1102 (1998).

7.   Allen, C.W., "Astrophysical Quantities" (Athlone Press, London), p.145, 1955.

8.   *ibid*., p.162.

9.   Bernstein, R.A., Friedman, W.L., and Madore, B.F., "The First Detections of the Extragalactic Background Light at 3000, 5500, and 8000 Å. II. Measurement of Foreground Zodiacal Light," Ap. J., vol. **571**, 85 (2002).

10.   Schwartz and Gursky, in 'X-ray Astronomy', eds. Giacconi and Gursky, (D. Riedel), 1974

11.   Snowden *et. al.*, Ap. J., vol. **454,** 643 (1995).